Murdoch
UNIVERSITY

MURDOCH RESEARCH REPOSITORY

This is the author's final version of the work, as accepted for publication following peer review but without the publisher's layout or pagination. The definitive version is available at
http://dx.doi.org/10.3850/978-981-07-5936-0_06-04

Ahubelem, N., Altarawneh, M. and Dlugogorski, B.Z. (2013) Kinetic and mechanistic study into emission of HCl in fires of PVC. In: Proceeding of the Seventh International Seminar on Fire and Explosion Hazards (ISFEH7), 5 - 10 May, Providence, RI, USA pp. 371-380.

http://researchrepository.murdoch.edu.au/22814/

Copyright: © 2013 University of Maryland.

It is posted here for your personal use. No further distribution is permitted.

Kinetic and Mechanistic Study into Emission of HCl in Fires of PVC

Ahubelem, N.*, Altarawneh, M., and Dlugogorski, B.Z.

Process Safety and Environment Protection Research Group
School of Engineering
The University of Newcastle, Callaghan NSW 2308, Australia
**Corresponding author email: Nwakamma.Ahubelem@uon.edu.au*

ABSTRACT

PVC pyrolyses in fires eliminating HCl, which can subsequently participate in formation of chloraromatic pollutants. In this study, the density functional theory (DFT) has been deployed to simulate the mechanisms of HCl elimination from pyrolysing PVC. Although PVC consists mainly of polymerised chlorethene, it also contains other structural entities as impurities or defect compounds, which significantly enhance its decomposition. For this reason, we have studied elimination of HCl from seven compounds that represent the defects in PVC. We have found two generic pathways for the elimination of HCl. The first involves a C-Cl fission at an allylic site and a C-H cleavage at a vinylic site, whereas the second entails scissions of allylic Cl and methylenic H. The latter pathway appears more favourable from thermodynamic and kinetic standpoints. We have investigated the effect of the length of carbon chain on reaction and activation enthalpies by considering analogous dehydrochlorination pathways for short chlorinated alkanes (i.e., C_3, C_4), discovering the reaction and activation enthalpies required for HCl elimination to be independent of the length of the carbon chain. We then explored the effects of temperature and pressure on rate constants for all possible dehydrochlorination pathways within the formalism of the unimolecular reaction rate theory of RRKM. Pressure fall-off regions extend generally between 0.001 and 1.0 atm, and the dehydrochlorination reactions exhibit pressure-independent behaviour even under ambient pressure. Kinetic parameters presented herein should be useful to model the decomposition of PVC in fires.

INTRODUCTION

Polyvinyl chloride (PVC) is widely used in buildings, floorings, home furnishings, electrical insulation, packagings, clothing and automobile parts, with HCl forming in fires of these materials. Elevated emissions of HCl have been measured from incineration[1] and pyrolysis[2] of materials that comprise PVC. Unimolecular elimination of HCl during thermal decomposition of chlorinated hydrocarbons has been the focus of increasing interests, in view of the nature of HCl as a toxic gas and its potent role in the formation of notorious chlorinated pollutants.

For instance, a study, involving non-flaming and flaming destruction of PVC from a window frame, demonstrated HCl to be the most abundant component of the evolved gas mixture[3]. A smoke releasing device and a Fourier transform infrared spectrometer (FTIR) were deployed to conduct a quantitative on-line analysis of the concentration of HCl in a smoke of PVC. Results showed that, although the concentration of HCl increased slightly during the flaming combustion of PVC, most of the HCl released (~80 %) and the highest smoke toxicity attained occurred before the onset of the flaming combustion[4].

In another study, it was found that, HCl emission accounts for 53 % of the mass of the entire PVC when 40 000 molecular weight PVC was pyrolysed in vacuum up to a temperature of 500 ˚C. PVC was observed to show two degradation stages[5]. Stage 1 involves the evolution of HCl and benzene simultaneously at temperatures typically between 200 and 360 ˚C. Stage 2 (360 to 500 ˚C) involves dehydrochlorination (relatively small amount of HCl in comparison to stage 1) and generation of alkyl aromatic and condensed ring aromatic hydrocarbons. Both stage 1 and stage 2 dehydrochlorination are initiated by the cleavage of tertiary chlorine atoms. Even though

Proc. of the Seventh International Seminar on Fire & Explosion Hazards (ISFEH7), pp. xx-xx
Edited by D. Bradley, G. Makhviladze, V. Molkov, P. Sunderland, and F. Tamanini
Copyright © 2013 University of Maryland. Published by Research Publishing
ISBN: 978-981-08-7724-8 :: doi: 10.3850/978-981-08-7724-8_0x-0x

the chlorines in PVC are in a secondary position, there could be deviations from the ideal structure and some of the chlorines can be in a tertiary position[5-6]. Dehydrochlorination from an ideal PVC structure leads to the formation of a double bond:

$$-[CH_2\text{-}CHCl\text{-}CH_2\text{-}CHCl]- \rightarrow -[CH_2\text{-}CHCl\text{-}CH{=}CH]- + HCl$$

Subsequently, the chlorine atom at the adjacent carbon atom becomes labile, with further HCl elimination leading to the formation of a new conjugated double bond and activation of other chlorine atoms. Based on this mechanism, HCl elimination proceeds at a fast rate, inducing the formation of conjugated double bonds.

However, mechanistic considerations, spectroscopic and chemical approaches disclose that PVC contains impurities such as chlorinated C_4-C_{10} aliphatics[7-8]. These impurities could be more thermally labile than the ideal PVC. The HCl elimination mechanisms of the short chain analogous species of some of these impurities have been earlier investigated by pristarino's group[9-10]. In the experiments performed by the later, they observed that in the absence of a tertiary carbon atom, C-Cl scission from a secondary carbon and the formation of a secondary carbenium ion dominates the initiation pathway for HCl elimination[9-10]. To this end, the present study investigates mechanisms of HCl elimination in PVC impurities as one of the pathways of the decomposition of PVC in fires. The primary aim is to provide kinetic and mechanistic insights into the decomposition behaviour of PVC.

MATERIALS, METHODOLOGY AND COMPUTATIONAL DETAILS

Geometrical optimisations and vibrational frequencies were calculated at the B3LYP6-311+G(D,P) level of theory. To provide a benchmark of the accuracy of this theoretical level, reaction and activation energies for 2-chloropropene were also estimated at the QB3, M052X/6-311+G(d,p) and G3B3 levels of theory. Calculations were carried out using the Gaussian 09[11] software. Effects of pressure and temperature changes on rate constants were thoroughly investigated based on the RRKM theory as implemented in the Chemrate code[12].

RESULTS AND DISCUSSION

Potential energy surfaces (PESs)

PVC consists of monomer units of chlorethens. However, PVC also contains other structural entities as impurities or defect compounds. Defect compounds are important in the decomposition of PVC. It is found that degradation of PVC is significantly enhanced by the presence of these defect compounds. Because of this consideration, we have studied the elimination of HCl from seven model compounds that represent the defects in PVC. These model compounds include 2-chlorodec-3-ene (*Z1*), 4-chlorodec-2-ene (*Z2*), 1-chloronon-2-ene (*Z3*), 4-chlorodec-2-ene (*Z4*), 6-chloronon-4-ene (*Z5*), 5-chloro-5-ethylnonane (*Z6*), and 1,3-dichlorononane (*Z7*). The compounds contain functional groups representative of the major defects in PVC. Compound *Z7* represents a simple segment of PVC while *Z6* contains a tertiary halogen. *Z1* to *Z5* represent the types of unsaturation which may be present. Similarly, the HCl elimination kinetics of 3-chlorobutene (*Y1*), 1,3-dichlorobutane (*Y7*), 2-chloropropene (*M1*), 1,3-dichlorpropene (*M2*), 2-chlorodecene (*X1*) and 1,3-dichlorodecene (*X2*) were studied to investigate the effect of the length of carbon chain on kinetic and thermodynamic features of the dehydrochlorination reactions. Table 1 lists the calculated reaction and activation enthalpies. The $\Delta H^{\ddagger}$ and $\Delta_r H$ values, calculated for *M1* by the composite method of CBS-QB3 and G3B3, are in very good agreement with the corresponding values calculated at the B3LYP/6-311+G(d,p) level of theory. On the other hand, the M052X/6-311+G(d,p) seems to underestimate significantly $\Delta H^{\ddagger}$ and $\Delta_r H$ values in reference to other methods.

Two possible pathways have been investigated. First pathway involves a C-Cl fission at an allylic site and a C-H cleavage at a vinylic site and the second entails a homolytic scission of C-Cl at an allylic site and fission of a methylenic hydrogen. Figure 1 maps out the potential energy surface (PES) for dehydrochlorination pathways for all the species involved. The initial decomposition of $C_{10}H_{17}Cl$ (*Z1*) produces two distinct moieties. C-Cl fission from the allylic site and the C-H fission from the vinylic site with a simultaneous HCl elimination is found to be endoergic by 22.2 kcal/mol and results in the formation of *P1*. C-Cl and C-H fissions from the allylic and methylenic sites, respectively, and HCl elimination represents the most favourable pathway with an endothermicity amounting to 9.7 kcal/mol and an enthalpic barrier of 35.2 kcal/mol, leading to the formation of *P2*. Similarly, the homolytic cleavage of the C-Cl bond from the allylic site of *Z2* and C-H scission from the vinylic site, resulting in formation of *P3* and HCl, were found to be endoergic by 21.6 kcal/mol. Scissions of the C-Cl bond and C-H bond at the allylic and methylenic sites and the formation of *P4* moiety with HCl elimination represents the most favourable pathway with an energy barrier of 34.4 kcal/mol and endothermicity of 6.3 kcal/mol. Compound *Z3* was found to have only one pathway for HCl elimination, which involved fission of C-Cl bond at the terminal allylic group and cleavage of the C-H bond at the vinylic site, resulting in *P5* formation and HCl elimination with an endothermicity of 20.8 kcal/mol.

The thermal dehydrochlorination of *Z4* was observed to follow two pathways. The first involves C-Cl and C-H scissions at the allylic and methylenic sites, respectively, forming *P6* with an activation energy of 32.5 kcal/mol. The second comprises fission of the C-Cl bond at the allylic site, C-H cleavage at the vinylic site and the resultant formation of *P7* moiety, upon elimination of HCl. *P6* pathway was found to be the most favourable with an endothermicity of 4.6 kcal/mol.

Table 1. Calculated reaction and activation enthalpies at 298.15 K for all reactions.

Reaction	Method	$\Delta H^{\ddagger}$ (kcal/mol)	$\Delta_r H$ (kcal/mol)
Z1→*P1*+HCl	B3LYP/6-311+G(d,p)		22.23
Z1→*P2*+ HCl	B3LYP/6-311+G(d,p)	35.24	9.70
Z2→*P4*+ HCl	B3LYP/6-311+G(d,p)	34.42	6.31
Z2→*P3*+ HCl	B3LYP/6-311+G(d,p)		21.60
Z3→*P5*+ HCl	B3LYP/6-311+G(d,p)		20.83
Z4→*P6*+ HCl	B3LYP/6-311+G(d,p)	32.47	4.56
Z4→*P7*+ HCl	B3LYP/6-311+G(d,p)		20.41
Z5→*P8*+ HCl	B3LYP/6-311+G(d,p)	34.46	6.38
Z5→*P9*+ HCl	B3LYP/6-311+G(d,p)		21.02
Z6→*P10*+ HCl	B3LYP/6-311+G(d,p)	32.40	7.76
Z7→*P11*+ HCl	B3LYP/6-311+G(d,p)	48.75	8.15
Z7→*P12*+ HCl	B3LYP/6-311+G(d,p)	40.47	6.89
Z7→*P14*+ HCl	B3LYP/6-311+G(d,p)	41.19	8.27
Y1→*R2*+HCl	B3LYP/6-311+G(d,p)	39.24	9.47
Y7→*R11*+ HCl	B3LYP/6-311+G(d,p)	43.35	8.21
Y7→*R12*+HCl	B3LYP/6-311+G(d,p)	43.48	7.06
Y7→*R14*+HCl	B3LYP/6-311+G(d,p)	43.35	10.28
M1→*PM1* + HCl	B3LYP/6-311+G(d,p)	58.47	24.81
M2→*PM2* + HCl	B3LYP/6-311+G(d,p)	69.62	26.08
X1→*PX1* + HCl	B3LYP/6-311+G(d,p)	54.22	21.89
X2→*PX2* + HCl	B3LYP/6-311+G(d,p)	67.09	26.16
M1→*PM1* + HCl	M052X/6-311+G(d,p),	43.51	29.75
M1→*PM1* + HCl	CBS-QB3	58.12	24.97
M1→*PM1* + HCl	G3B3	61.53	32.49

Fissions of the allylic C-Cl and methylenic C-H bonds, and the formation of *P8* with HCl elimination, dominate the initial decomposition of compound *Z5*. The reaction was found to be endoergic by 6.4 kcal/mol with a barrier of 34.5 kcal/mol.

Thermal dehydrochlorination of compound *Z6* was observed to follow one major pathway of the formation of *P10* structure via the C-Cl and C-H cleavages at the methylenic sites with an activation enthalpy of 32.4 kcal/mol and endothermicity of 7.8 kcal/mol. Compound *Z7* was found to follow three major pathways of thermal dehydrochlorination. These pathways involve a C-H fission at methylenic sites and the formation of *P11*, *P12* and *P14* moieties through activation enthalpies of 48.7, 40.5 and 41.2 kcal/mol and endothermicities of 8.1, 6.9 and 8.3 kcal/mol, respectively. The formation of *P12* represents the most favourable pathway with an endothermicity of 6.9 kcal/mol. Even though *Z6* has a tertiary Cl, there is no other Cl atom in *Z6* for us to compare the HCl elimination. However, we observed that *Z6* has the least activation enthalpy. This implies that a tertiary Cl atom could be a major initiator of the dehydrochlorination in PVC in accordance with experimental observations of McNeil's group[5]and Hjeertbeert group[6] mentioned earlier. In addition, compound *Z7* and *Y7* has no tertiary carbon atoms but secondary and primary chlorine atoms. C-Cl scission via the secondary carbon atom and the formation of their respective compound *P12* and *R12* with relatively lower endothermicity among other optimized product species (*P11, P14* and *R11, R14*) indicates that in the absence of a tertiary chlorine atom, chlorine atoms at the secondary position are more important initiation sites for dehydrochlorination than their primary equivalents. This is in agreement with the experimental findings of Pistarino's group[9-10] mentioned earlier.

We investigated the effect of the length of carbon chain on HCl elimination reactions by comparing the reaction and activation enthalpies between short-chain (*Y1* and *Y7*) and their analogous long-chain (*Z1* and *Z7*) chlorinated hydrocarbons. In addition, single-pathway dehydrochlorination reactions of 2-chloropropene (*M1*) and 1,3-dichloropropene (*M2*) were compared to their respective analogous long chain (*X1* and *X2*) dehydrochlorination reactions as illustrated in Figure 1.

We found that compound *Y1* with shorter carbon chain undergoes a HCl elimination reaction to yield *R2* with a barrier of 39.2 kcal/mol and an endothermicity of 9.5 kcal/mol, while the analogous long chain compound (*Z1*) eliminates HCl to yield *P2*, with a barrier of 35.2 kcal/mol and endothermicity of 9.7 kcal/mol, as was shown earlier. Similarly, compound *Y7* expels HCl to yield *R11*, *R12* and *R14* with activation enthalpies of 43.4, 43.5 and 43.4 kcal/mol and endothermicities of 8.2, 7.1 and 10.3 kcal/mol, in that order. The long chain analogous species of *Y7* (*Z7*) were earlier shown to undergo the same reaction with barriers of 48.7, 40.5 and 41.2 kcal/mol and corresponding endothermicities of 8.1, 6.9 and 8.3 kcal/mol.

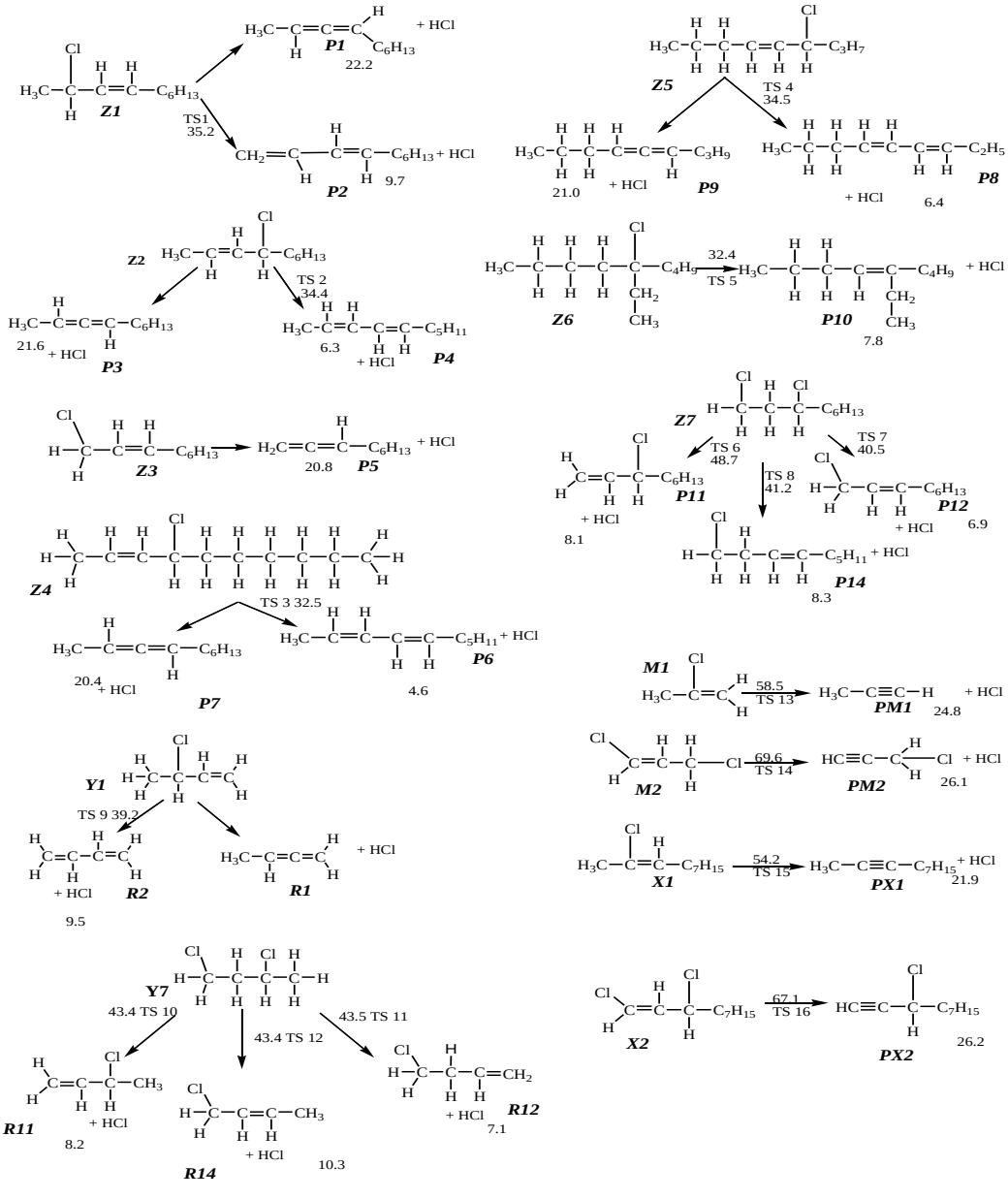

Figure 1. PES for the thermal dehydrochlorination of 2-chlorodec-3-ene (*Z1*), 4-chlorodec-2-ene (*Z2*), 1-chlorononon-2-ene (*Z3*), 4-chlorodec-2-ene (*Z4*), 6-chlorononon-4-ene (*Z5*), 5-chloro-5-ethylnonane (*Z6*), 1,3-dichlorononane (*Z7*), 3-chlorobutene (*Y1*), 1,3-dichlorobutane (*Y7*), 2-chloropropene (*M1*), 1,2-dichlorpropene (*M2*), 2-chlorodecene (*X1*) and 1-chlorodecene (*X2*). Values in bold and italic (in kcal/mol at 298.15 K) refer to reaction and activation enthalpies, respectively.

The HCl eliminations from 2-chloropropene (*M1*) and 1,3 dichloropropene (*M2*) were found to be endoergic by 24.8 and 26.1 kcal/mol respectively, with the corresponding barriers of 58.5 and 69.6 kcal/mol. This is comparable to the HCl elimination from their analogous long-chain compounds *X1* and *X2*, with endothermicities of 21.9 and 26.2 kcal/mol and activation enthalpies

of 54.2 and 67.1 kcal/mol, respectively. Thus, with all other parameters kept constant (e.g. fixed position and number of Cl and H atom), the reaction and activation enthalpies required for HCl elimination are independent of the length of the carbon chain. Generally, we could not optimise the transition states (TS) for the formation of C=C=C. The TS are composed of atoms Cl_1, C_2, C_3 and H_4, with structures characterised by four centred geometries. The numbering scheme for the four-centred TS geometry is obeyed by all the optimised reactants, transition states and products in clockwise direction for *Z1-P2TS*, *Z5-P8TS*, *Z6-P10TS*, *Z7-P12TS*, *Y7-R11TS* and *X1-PX1TS*. The Cl_1, C_2, C_3 and H_4 numbering system is also obeyed by other optimised structures in the anticlockwise direction for *Z2-P4TS*, *Z4-P6TS*, *Z7-P14TS*, *Y1-R2TS*, *Y7-R14TS*, *Y7-R11TS*, *M1-PM1TS*, *M2-PM2TS* and *X2-PX2TS*. Geometries of transition structures for all reactions are sketched in Fig. 2. Prominent structural parameters of reactants, transition structures, and products are reported in Table 2.

Substantial increase of Cl_1-C_2 distance from about 1.7-1.8 Å to 2.5-2.9 Å was observed for all substrates, demonstrating the breaking of Cl_1-C_2 bond in the TS. The distance C_2-C_3 is reduced from 1.5 to 1.4 Å in the TS validating double bond formation. *M1*, *M2*, *X1* and *X2* in dehydrochlorination reactions have their C_2-C_3 distance reduced from 1.3 to 1.25-1.26 Å, indicating triple bond formation. The C_3-H_4 bond elongation in the TS is significant from 1.08-1.09 to 1.17-1.25 Å. This is because the hydrogen atom H_4 is approaching closer to Cl_1 to form hydrogen chloride and hence, H_4-Cl_1 distance decreases from 2.8-3.0 Å in the reactant to 1.8-2.0 Å in the TS.

Reaction rate constants

Modified Arrhenius parameters for apparent dehydrochlorination reactions at 1 atm and at the high-pressure limit are given in Table 3. To the best of our knowledge, there are no experimental measurements for dehydrochlorination for the seven targeted model PVC compounds. However, experimental measurements along with theoretically-based values[13] exist for 2-chloropropene. In Table 4, we compare our estimated rate constants from different theoretical methods with the corresponding experimentally derived rate parameters.

Our estimated E_a values agree satisfactorily with the corresponding experimental measurement, except for that computed by the M052X/6-311+G(d,p) method, which yielded a somewhat underestimated prediction. Effects of temperature and pressure on rate constants for all possible dehydrochlorination pathways were investigated within the formalism of the unimolecular reaction rate theory of RRKM. Pressure fall-off regions extend generally between 0.01 and 1.0 atm for 1,3-dichlorononane (*Z7*), as shown in Fig. 3. The pressure fall-off region of the short-chain analogous compound of 1,3-dichlorononane (1,3-dichlorobutane (*Y7*)) stretches to between 0.001 and 1 atm (Fig. 4), which is the same as that of 1,3-dichloropropene (*M2*, not shown). Figures 5 and 6 demonstrate the calculated Arrhenius plots for reaction rate constants for the three available dehydrochlorination pathways for 1,3-dichlorononane and 1,3-dichlorobutane at 1.0 atm, relevant to conditions in fires. It is found that, dehydrochlorination reactions exhibit pressure-independent behaviour even under atmospheric pressure.

CONCLUSIONS

HCl elimination in PVC fires was studied to develop a practical reaction mechanism. We found that the HCl elimination pathways fall into one of two schemes. The first involves a homolytic C-Cl fission at an allylic site and a C-H cleavage at a vinylic site and the second entails C-Cl and C-H scissions at allylic and methylenic sites, respectively. Tertiary Cl atom represents the dominant initiation site in HCl elimination in PVC laden with impurities. In the absence of a tertiary Cl atom, secondary Cl atoms dominate HCl elimination pathway. With other parameters (such as

position and number of Cl and H atoms kept constant), the enthalpies and activation enthalpies required for HCl elimination are independent of the length of the carbon chain. Kinetic parameters tabulated in the contribution could be included in models of the decomposition of PVC in fires and in other thermal processes containing aliphatic chlorinated compounds.

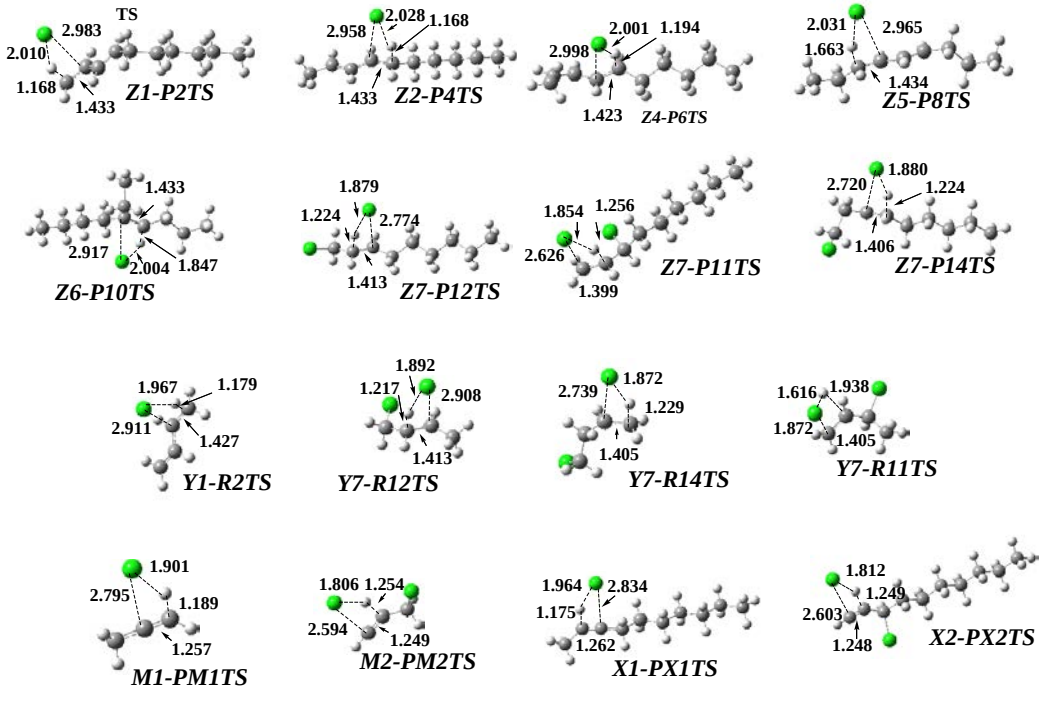

Figure 2. Optimised structures for transition state TS in the gas phase elimination of HCl from PVC model compounds (2-chlorodec-3-ene (*Z1*), 4-chlorodec-2-ene (*Z2*), 1-chloronon-2-ene (*Z3*), 4-chlorodec-2-ene (*Z4*), 6-chloronon-4-ene (*Z5*), 5-chloro-5-ethylnonane (*Z6*), 1,3-dichlorononane (*Z7*)), selected chloro alkanes and alkenes (3-chlorobutene (*Y1*), 1,3-dichlorobutane (*Y7*), 2-chloropropene (*M1*), 1,2-dichlorpropene (*M2*), 2-chlorodecene (*X1*) and 1-chlorodecene (*X2*)) at B3LYP/6-311+G(d,p)

Table 2. Structural parameters of reactant (R), transition state (TS), and products (P) for HCl elimination from PVC model compounds (*Z1-Z7*) and selected chloroalkanes and chloroalkenes (*Y1*,*Y7*, *M1*, *M2*,*X1* and *X2*).

		Atomic Lengths (Å)			
Reactions		Cl_1-C_2	C_2-C_3	C_3-H_4	H_4-Cl_1
Z1→*P2*+ HCl	R	1.862	1.522	1.095	2.903
	TS	2.983	1.433	1.168	2.009
	P		1.339		
Z2→*P4*+ HCl	R	1.863	1.528	1.095	3.050
	TS	2.958	1.433	1.168	2.028
	P		1.341		
Z4→*P6*+ HCl	R	1.864	1.528	1.095	3.059
	TS	2.998	1.423	1.194	2.001
	P		1.341		
Z5→*P8*+ HCl	R	1.863	1.528	1.095	3.059
	TS	2.965	1.434	1.194	2.001
	P		1.341		
Z6→*P10*+ HCl	R	1.876	1.539	1.095	2.862
	TS	2.917	1.433	1.847	2.004
	P		1.340		
Z7→*P11*+ HCl	R	1.819	1.532	1.093	2.782
	TS	2.626	1.399	1.256	1.854
	P		1.330		
Z7→*P12*+ HCl	R	1.838	1.528	1.093	3.008
	TS	2.774	1.413	1.224	1.879
	P		1.334		
Z7→*P14*+ HCl	R	1.838	1.528	1.093	3.008
	TS	2.774	1.413	1.224	1.879
	P		1.334		
Y1→*R2*+HCl	R	1.854	1.522	1.092	3.024
	TS	2.911	1.427	1.179	1.967
	P		1.338		
Y7→*R11*+ HCl	R	1.818	1.529	1.093	2.808
	TS	1.872	1.405	1.938	1.616
	P		1.331		
Y7→*R12*+HCl	R	1.835	1.527	1.093	3.000
	TS	2.908	1.413	1.217	1.892
	P		1.334		
Y7→*R14*+HCl	R	1.835	1.522	1.093	2.966
	TS	2.739	1.405	1.229	1.872
	P		1.331		
M1→*PM1* + HCl	R	1.773	1.327	1.081	2.849
	TS	2.795	1.257	1.189	1.901
	P		1.202		
M2→*M2* + HCl	R	1.744	1.328	1.084	2.887
	TS	2.594	1.249	1.254	1.806
	P		1.201		
X1→*PX1* + HCl	R	1.779	1.331	1.089	3.693
	TS	2.603	1.262	1.249	1.812
	P		1.205		
X2→*PX2* + HCl	R	1.747	1.328	1.085	2.888
	TS	2.603	1.248	1.249	1.812
	P		1.202		

Table 3. Kinetic and Arrhenius parameters of HCl elimination at 300-2000 K

Reactions	Method	At 1 atm			At high pressure		
		A (s^{-1})	E_a (kcal/mol)	n	A (s^{-1})	E_a (kcal/mol)	n
Z1→*P2*+HCl	B3LYP/6-311+G(d,p)	1.57×10^{63}	50.38	-15.46	5.87×10^{12}	35.60	0.60
Z2→*P4*+HCl	B3LYP/6-311+G(d,p)	5.45×10^{48}	46.15	-10.89	2.14×10^{12}	34.80	0.58
Z4→*P6*+HCl	B3LYP/6-311+G(d,p)	1.37×10^{38}	44.12	-7.73	1.75×10^{11}	35.54	0.67
Z5→*P8*+HCl	B3LYP/6-311+G(d,p)	4.3×10^{55}	47.78	-13.09	3.93×10^{12}	34.87	0.56
Z6→*P10*+HCl	B3LYP/6-311+G(d,p)	1.5×10^{61}	46.40	-14.99	5.73×10^{12}	32.75	0.63
Z7→*P11*+HCl	B3LYP/6-311+G(d,p)	2.8×10^{58}	64.32	-13.97	2.8×10^{58}	64.32	-13.97
Z7→*P12*+HCl	B3LYP/6-311+G(d,p)	8.45×10^{49}	52.83	-11.38	8.45×10^{49}	52.83	-11.38
Z7→*P14*+HCl	B3LYP/6-311+G(d,p)	2.35×10^{49}	52.44	-11.57	2.35×10^{49}	52.44	-11.57
Y1→*R2*+HCl	B3LYP/6-311+G(d,p)	7.75×10^{40}	48.57	-8.50	1.03×10^{12}	39.57	0.64
Y7→*R11*+ HCl	B3LYP/6-311+G(d,p)	6.98×10^{37}	52.08	-7.48	2.29×10^{11}	43.58	0.85
Y7→*R12*+HCl	B3LYP/6-311+G(d,p)	7.86×10^{38}	52.54	-7.80	1.9×10^{11}	43.72	0.87
Y7→*R14*+HCl	B3LYP/6-311+G(d,p)	1.4×10^{38}	52.15	-7.58	2.29×10^{11}	43.58	0.85
M1→*PM1* + HCl	B3LYP/6-311+G(d,p)	1.56×10^{33}	65.68	-5.86	4.8×10^{11}	58.74	0.89
M2→*PM2* + HCl	B3LYP/6-311+G(d,p)	1.52×10^{28}	75.40	-4.20	1.52×10^{11}	69.82	1.11
X1→*PX1* + HCl	B3LYP/6-311+G(d,p)	6.78×10^{34}	62.15	-6.22	1.18×10^{12}	54.56	0.81
X2→*PX2* + HCl	B3LYP/6-311+G(d,p)	8.87×10^{22}	71.32	-2.51	1.38×10^{11}	67.29	1.11
M1→*PM1* + HCl	M052X/6-311+G(d,p),	4.96×10^{41}	53.00	-8.67	1.69×10^{11}	43.73	1.01
M1→*PM1* + HCl	CBS-QB3	2.97×10^{33}	65.42	-5.95	4.66×10^{33}	58.40	0.90
M1→*PM1* + HCl	G3B3	1.19×10^{32}	68.39	-5.48	5.69×10^{11}	61.81	0.88

Table 4. Arrhenius parameters for the decomposition of alkyl chloride at high pressure.

Reactions	Method	Log A (s^{-1})	*Ea* (kcal/mol)	Ref.
2-C_2H_5Cl→HCl+C_3H_4	Experimental	13.05	57.9	[13]
2-C_2H_5Cl→HCl+C_3H_4	B3LYP/6-311+G(d,p)	11.68	58.74	[a]
2-C_2H_5Cl→HCl+C_3H_4	M052X/6-311+G(d,p)	11.23	43.73	[a]
2-C_2H_5Cl→HCl+C_3H_4	CBS-QB3	11.67	58.40	[a]
2-C_2H_5Cl→HCl+C_3H_4	G3B3	11.76	61.81	[a]
*C_2H_3Cl→HCl+C_2H_2	Experimental	14	69.2	[14]

[a] This work
* Vinyl Chloride

REFERENCES

1. Lew, G., "Preliminary Test Data from the Modesto Energy Company Evaluation Test", California Air Resources Board Sacramento, 1990.
2. Kuramochi, H., Wu, W., Kawamoto, K., "Study on HCl Emission Behaviour During Pyrolysis of Demolition Wood with PVC and Municipal Solid Waste for Clean Hydrogen Production", Proc. World Hydrogen Energy Conf. 16, 13-16 (2006).
3. Alajbeg, A., "Products of Non-flaming Combustion of Poly (Vinyl Chloride)", J. Anal. Appl. Pyrolysis 275-291 (1987).
4. Chunsheng, J.I., Zian, L.U., Chenzhou, L., et al., "The Release Pattern of HCl from the Combustion of PVC", Acta Polym. Sin. 1, 674-677 (2005).
5. McNeill, C.I., Memetea, L., and William, J.C., "A Study of the Products of PVC Thermal Degradation", Polym. Degrad. Stabil. 181-191 (1995).
6. Hjeertberg, T., and Sorvik, E.M., "*Degradation and Stabilisation of PVC*", Owen, E.D. (ed.), Elsevier, London, 1984, p. **21**/320.

7. Hjeertberg, T., and Sorvik, E.M. "Formation of Anomalous Structures in PVC and Their Influence on Thermal Stability. I. Endgroup Structures and labile Chlorine Substituted by Phenol", J. Macromol. Sci., Chem., 17:983 (1982).
8. Guyot, A., "Recent Developments in the Thermal Degradation of Polystyrene-A Review", Polym. Degrad. Stabil., 15:219-235 (1986).
9. Pistarino, C., Finocchio, E., Larrubia, M. A., Serra, B., Braggio, S., and Busca, G., "A Study of the Dehydrochlorination of 1, 2-Dichloropropane over Silica-Alumina Catalysts", Ind. Eng. Chem. Res., 40:3262-3269 (2001).
10. Pistarino, C., Finocchio, E., Romezzano, G., Brichese, F., Di Felice, R., and Busca, G., "A Study of the Catalytic Dehydrochlorination of 2-Chloropropane in Oxidizing Conditions", Ind. Eng. Chem. Res., 39:2752-2760 (2000).
11. Frisch, M.J., Trucks, G.W., Schlegel, H.B., Scuseria, G.E., Robb, M.A., Cheeseman, J.R., et al., "Gaussian 09, rev. A 01", Gaussian Inc., Wallingfort CT, 2009.
12. Mokrushin, V., Bedanov, V., Tsang, W., Zachariah, M., Knyazev, V., "ChemRate, ver 1.19", NIST Gaithersburg, MD, USA 2002.
13. Nisar, J., and Awan, I. A., "A Gas Phase Kinetic Study on the Thermal Decomposition of 2-Chloropropene", Kinetics and Catalysis 49:461-465 (2008).
14. Manion, J.A., and Louw, R., "Gas Phase Hydrogenolysis of Chloroethene: Rates, products and Computer Modelling", J. Chem. Soc., Perkin Trans. 2, 1547-1555 (1988).

ACKNOWLEDGEMENTS

This study was supported by a grant from the Australian Research Council. NA thanks the University of Newcastle, Australia for a postgraduate research scholarship.

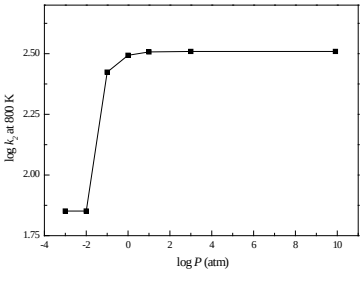

Figure 3. Pressure fall-off region for 1,3-dichlorononane at 800 K.

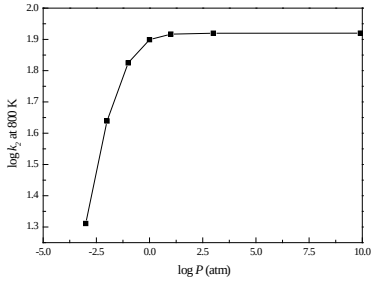

Figure 4. Pressure fall-off region for 1,3-dichlorobutane at 800 K.

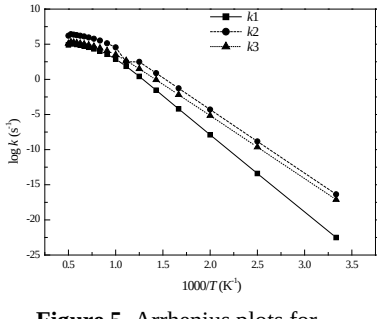

Figure 5. Arrhenius plots for dehydrochlorination reactions of 1,3-dichlorononane at 1.0 atm.

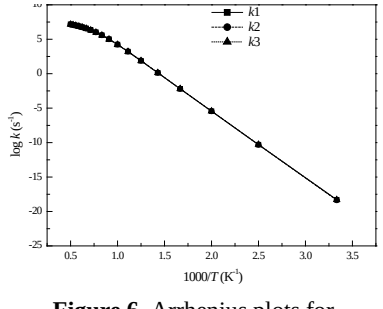

Figure 6. Arrhenius plots for dehydrochlorination reactions of 1,3-dichlorobutane at 1.0 atm.